BNWL-SA-5735

CONF-760858--1

Nodular Corrosion of the Zircaloys

For presentation at the Symposium,
Zirconium in the Nuclear Industry
Quebec, Canada August 10-12, 1976

by
AB Johnson,Jr.
RM Horton

August, 1976

BATTELLE
Pacific Northwest Laboratories
Richland, Washington 99352

This work was done for the Energy Research and Development Administration under contract E(45-1): 1830

DISCLAIMER

BNWL-SA-5735

Nodular Corrosion of the Zircaloys

A. B. Johnson, Jr.

Corrosion Research and Engineering Section
Battelle Northwest
Richland, Washington 99352

R. M. Horton*

Materials Research Section
Aerojet Nuclear Co.
Idaho Falls, Idaho 83401

*Work performed while on a NORCUS assignment (ERDA-sponsored summer employment) at Battelle Northwest.

Paper for presentation at the symposium "Zirconium in the Nuclear Industry", Quebec, Canada, August 10-12, 1976.

Abstract

Nodular Corrosion on the Zircaloys

A.B. Johnson, Jr.[1] and R.M. Horton[2]

Oxide nodules form on Zircaloy nuclear components under irradiation. Similar nodules were observed on Zircaloy coupons in cold rolled or extended conditions after autoclave treatments at 475°C and 500°C in steam at 1500-1700 psi. The stages of nodular corrosion in the autoclave were: nodule nucleation, growth, coalescence, propagation to accelerated uniform corrosion, and complete specimen oxidation. Observations on BWR fuel rods suggest that a similar progressive attack has occurred; however, in no case has the in-reactor attack progressed to the stage of complete fuel rod failure.

Recent autoclave tests confirmed the nodular character of the attack on cold worked materials. Alpha anneals (up to 790°C) did not consistently suppress the nodular attack. However, alpha + beta (840°C) and beta (1010°C and 1040°C) anneals did suppress the attack if followed by a fast cool. The efficacy of the anneals applied similarly to Zircaloy-2 and Zircaloy-4. Stresses associated with U-bend specimens and heavy (86%) cold work did not enhance the nodular attack before stress relief occurred.

---

[1]Corrosion Research and Engineering Section, Battelle Northwest, Richland, Washington 99352.

[2]Materials Science Branch, Acrojct Nuclear Co., Idaho Falls, Idaho 83401. Work completed while on a NORCUS appointment at Battelle Northwest.

Additional work is required to confirm preliminary evidence that materials in the reactor and autoclave environments respond similarly to factors such as metallurgical conditions.

The nodular attack on reactor components appears to depend on nuclear flux, and develops in oxygenated reactor coolants, principally in the vicinity of fuel rod spacers. Experience with irradiated specimens in reactor loops suggests that uniform concentrations of dissolved oxygen alone do not initiate nodular attack.

Localized water chemistry associated with flow disturbances or, in some cases, dissimilar metals in fuel spacers, may be factors in the nodular attack in-reactor.

Nodular Corrosion of the Zircaloys

Introduction

Zircaloy-2[1] and Zircaloy-4[1] are the standard fuel cladding materials for nearly all water-cooled nuclear reactors produced in the Western world. Except for some early crud-induced failures, corrosion of the Zircaloys from the coolant side has not been a significant cause of fuel failures. However, accelerated corrosion, both uniform and localized, occurs on Zircaloy reactor components. The accelerated attack is most pronounced in the oxygenated boiling water reactor (BWR) coolants. A detailed description of the phenomena will not be repeated here, since that is well-documented. The phenomena most significant to this discussion are

- o oxide nodules[2] on BWR fuel cladding (Zircaloy-2) [1-3]; in some areas the nodules appear to have coalesced [1];
- o thick, spalling oxides on BWR fuel channels [4,5]; verbal descriptions suggest that the thick oxides initiated by a nodular mechanism;
- o nodular corrosion on fuel rods exposed in the Steam Generating Heavy Water Reactor (SGHWR), enhanced by proximity to fuel spacers, particularly at the inlet end [3];
- o nodular corrosion on KWO (PWR) Core One fuel rods, corresponding to a period of relatively high oxygen concentration in the primary coolant [6].

---

[1] Zircaloy-2 Zr, 1.5 Sn, 0.14 Fe, 0.1 Cr, 0.05 Ni
Zircaloy-4 Zr, 1.3 Sn. 0.22 Fe, 0.1 Cr, 0.007 Ni

[2] In this discussion nodules are defined as solid, lenticular localized oxide growths; pustules, as used here, differ by being substantially hollow.

Other instances of localized corrosion are reported under PWR conditions [7,8], but PWR experience generally indicates absence of oxide nodules and significant flux-enhanced corrosion [9].

Even though the localized corrosion has not caused fuel failures, the relatively thick nodular oxide on fuel rods and the thick, spalling oxide on fuel channels provide substantial incentive to understand the accelerated corrosion, the factors which accelerate and suppress it, and the potential consequences.

Relation to Experience with Non-Fueled Irradiated Specimens

Visual and microscope examinations on numerous specimens irradiated in reactor loops have revealed several instances of localized corrosion phenomena, including pustules [10, 11], localized surface roughening and associated oxide porosity [12], and alloy element segregation [10]. Corrosion in the vicinity of dissimilar metals also has resulted in local oxide thickening [11, 12]. However, oxide growth on the Zircaloys under irradiation did not involve nucleation of large oxide nodules in ETR [13, 14] or ATR [11] loop tests, even in oxygenated coolants. Oxide films from ~1um to ~150 um were essentially free of large oxide nodules [13, 14]. Van der Linde [15] observed pustules (nodules by the definition used here) on irradiated specimens in an oxygenated coolant, but in a region of flow disturbance. Thus, flow disturbances appear to be a major factor in the occurence of nodular corrosion in-reactor, perhaps creating localized water chesmistries in constrast to more uniform chemistries in the loop tests.

Dissimilar metals in fuel rod spacers (Inconel springs and, in some cases, stainless steel members) need to be considered in assessing nucleation of nodules on fuel rods.

Oxide spallation occurred occasionally, but was not a familiar phenomenon on reactor loop specimens, except at sharp corners on specimens having thick oxides [13].

Autoclave Studies of Nodular Corrosion

Oxide nodules nucleated on rolled or extruded Zircaloy-2 specimens exposed in high-pressure steam (1500-1700 psi) at 475 and 500°C [16]. The stages of the attack appear in Fig. 1, indicating that the nodular corrosion propagated to rapid general corrosion, which frequently nearly consumed specimens 0.75 mm thick within 24 hr at 500°C. The nodular attack was completely eliminated by a beta anneal (1010°C, 10-15 min), allowing the specimens to survive exposures of ~80 days at 500°C. Alpha anneals (760°C, 8 hr) suppressed nodules on the coupons, but oxide spalled more readily than on corresponding beta-annealed specimens. Beta anneals always suppressed the nodules on ~10 lots of Zircaloy-2 in approximately a dozen separate autoclave runs. Alpha anneals did not always suppress the nodules.

Several investigators (Referenced in 16) have seen the rapid approach to failure on Zircaloy-2 in high-pressure steam at ~500°C, but did not report nodular corrosion. To identify the nodular attack requires specimen inspection in early stages, before the nodules coalesce.

Cox [17] did not observe nodules on Zircaloy-2 specimens having alpha and beta anneals exposed at 500°C and 600°C in steam at 15, 500, 3000, and 5000 psi. However, his study did not include extruded or rolled specimens, which were most prone to develop nodules in the BNW studies. Cox's conditions spanned, but did not include, the pressure range used in the BNW studies.

Further work was performed at BNW to confirm that the earlier responses were reproducible, to extend the work to Zircaloy-4, and to investigate in more detail heat treatment effects.

Experimental

Three lots of Zircaloy-2 and one lot of Zircaloy-4 were included in the autoclave tests discussed here. The specimens were cleaned in detergent and acetone, vacuum heat treated (Table 2), pickled (57 vol % H_2O, 4 vol % HF, 39 vol % HNO_3), rinsed in $Al(NO_3)_3$, water and acetone.

The specimens were exposed in a stainless steel autoclave (5ℓ) on a stainless steel rack, at 475 or 500°C, in a steam pressure of 11 MPa (1600 psig). The autoclave feedwater was deionized (resistivity, ~1MΩ, and deoxgygenated (<0.1 ppm O_2). The refreshment rate was 1.2 ℓ/hr. The autoclave was vented upon startup to remove air, using standard methods [18].

The specimens were exposed in duplicate in each of the metallurgical conditions shown in Table 2, for 16 hr. at 500°C or for a succession of 8,8 and 16 hr. (total of 32 hr.) runs at 475°C. In addition, coupons of Zircaloy-2 lot HT [Refs 10, 14], having 86% cold work were exposed at 475°C and 500°C. U-bend specimens (one cm bend radius) were prepared from coupons of Zircaloy-2, lot 28787 and Zircaloy-4 lot 904. The specimens were autoclaved only at 500°C.

Results

The autoclaved specimens were characterized by visual and microscopic inspection, weight change, scanning electron microscopy (SEM) and metallography. The 500°C test, being more severe, was a better measure of the approach to failure, as a function of lot and heat treatment. The 475°C test was milder, providing opportunity for observations regarding nucleation of the nodules.

Visual Inspection

Figures 2 and 3 show specimens from 475°C and 500°C autoclave tests. Nodular corrosion of the type previously reported is clearly evident, in various stages of development. The severity of the attack varied from lot-to-lot and as a function of heat treatment. Zircaloy-2 and Zircaloy-4 corrosion responses differed in some details, but were similar in most aspects. The corrosion behavior of duplicate specimens was remarkably similar, in agreement with earlier results [16].

Effects of Heat Treatment

The principal observations regarding heat treatment effects are summarized below:

- The alpha treatments caused some improvements in resistance to nodular attack, but the influence was minimal for two Zircaloy-2 lots; the alpha anneals did not fully suppress the nodules on any lot. Anneals in the high alpha are marginally effective, generally improving resistance to nodular corrosion, sometimes suppressing nodules [16], but never as consistently as the beta anneal, fast cool.

- The alpha + beta, fast cool condition suppressed nodules and resulted in weight gains which were essentially the same as those on specimens in the beta anneal, fast cool condition.
- The beta anneal, fast cool conditions suppressed the nodular attack, though small areas of white oxide appeared on some specimens; weight gains were consistently low on beta, fast-cooled specimens.
- The beta anneal, slow cool, promoted nodules on all three Zircaloy-2 lots. The unfavorable effect of the slow cool was less for Zircaloy-4 than for Zircaloy-2 in both autoclave treatments.

Weight Changes

The weight changes on specimens in the two autoclave tests (Table 3) generally reflected the visual appearance. The relative order of the weight gains is summarized below:

Zircaloy-2 and Zircaloy-4:

$$500^{\circ}C: \text{As-rec}^{1} > \text{alpha} > \text{beta (slow)} > \frac{\text{alpha + beta}}{\text{beta (fast)}}$$

Zircaloy-2:

$$475^{\circ}C: \text{beta (slow)} > \frac{\text{alpha}}{\text{as-rec}} > \frac{\text{alpha + beta}}{\text{beta (fast)}}$$

Zircaloy-4:

$$475^{\circ}C: \text{as-rec} > \text{alpha} > \text{beta (slow)} > \frac{\text{alpha + beta}}{\text{beta (fast)}}$$

---

[1] Exception: Lot 1021 Zircaloy-2

Effect of Stress

U-bend and heavily cold worked (86%) specimens were included in the 500°C test to determine whether the stresses would influence nodule nucleation before stress relief occurred during the autoclave test. The post-test appearance of the U-bend specimens was similar to unstressed specimens of the same lot (38499). Heavy cold work also did not appear to accelerate nodule nucleation beyond what was expected. In the earlier study [16], nodules formed preferentially around intentional indents.

Microscopy

Figure 4 shows top views of mature nodules and several locations where nodules are nucleating. In advanced stages of coalescence, large cracks appeared in most of the "valleys" between adjacent nodules. A finer, layered crack structure developed within each nodule. The cracks were circumferential, centered on the upper tip of the nodule. A scanning microscopy view of a nodule pair emphasizes the layered structure of the intra-nodular crack pattern (Fig. 5). Localized corrosion on the beta slow-cooled specimens (Figure 4c) differed from the nodules on as-received and alpha-annealed specimens. The oxide mounds on the beta structures had transverse rather than circumferential cracks and were not cone-shaped.

Metallography

Figure 6 shows cross sections of nodules at several stages. The cracked nature of the oxide is evident, with cracks running roughly parallel to the metal/oxide interface. The tips of the nodules sometimes spalled, but otherwise they remained hard, tenacious and free of spallation.

Studies of the metallographic structures of the four materials used in this study is only partially complete.

Discussion

The autoclaved study reported here confirms the reproducibility of the nodular attack reported earlier [16]. However, it indicates that alpha anneals are not a dependable method to suppress nodules, but that alpha + beta and beta anneals suppress nodules if followed by a fast cool. It also indicates that Zircaloy-4 responds favorably to alpha + beta and beta anneals.

Comparison of In-Reactor and Out-of-Reactor Nodule Attack

The phases of the nodular attack indicated in Figure 1 appear to apply both to in-reactor and autoclave nodule development. Individual nodules have nucleated and grown to maturity on fuel rods (e.g., Figure 63 of Reference [1]). Some areas on fuel rods have thick oxides which likely resulted from nodule coalescence (e.g., Figure 63 of Reference [1]). Oxide spallation is reported to occur on BWR fuel rods, but we are not aware of any instance where the attack progressed to Stage e on in-reactor components.

The factors which promote the nodular attack in-reactor appear to be high system pressure, radiation, flow disturbances and oxygenated conditions. While the nodules frequently develop in the vicinity of dissimilar metals (spacers) there is no clear evidence that metal couples are a factor.

In the autoclave, the rapid attack at temperatures near 500°C increases with increasing steam pressure. The nodular corrosion initiates in-reactor in high-pressure water, but the autoclave and reactor environments have little in common.

On the other hand, similarities in the responses of materials to the two environments appear to be emerging. There are visual reports that welds on fuel channels are far more resistant to accelerated attack than the remainder of the fuel channels, appearing to parallel the efficacy of beta anneals in autoclave studies. There is preliminary evidence from our autoclave tests that the Zr-2.5Nb alloy in the quenched, cold work, aged condition resists nodular attack. Evidence from SGHWR observations suggests that the alloy resisted nodular attack under in-reactor conditions which produced it on Zircaloy [3].

If it can be demonstrated that the autoclave tests produce nodules reproducibly from lab to lab, and given materials respond similarly in autoclave and reactor environments, then the autoclave test may provide valuable insights to susceptibility to nodule development in-reactor.

Mechanisms

The state of understanding regarding the stages of nodular attack shown in Figure 1 are briefly outlined below.

Stage a

The factors which cause nodules to nucleate are not well understood for reactor or autoclave environments. Nodule nucleation involves a factor which causes corrosion to penetrate locally into the metal surface. The evidence that metallurgical factors are involved in the autoclave test are a) reproducible suppression of

nodules with selected heat treatments; b) reproducible nodule morphology on a given Zircaloy lot, but differing morphologies between lots.

Certain types of stressed areas appear to promote nodules [16], but stress does not appear to be first order factor.

Surface contaminants have been suggested as an explanation for the localized attack [4, 17]. However, if present, contaminant effects are clearly superimposed on metallurgical effects.

Local variations in dissolved alloy content or second phase particle distribution are two potential explanations for local corrosion penetrations.

Stage b

Once local incursions of oxide develop in the metal, the nodular corrosion appears to have the essentials of self-propagation. The oxide volume is ~1.5 times the volume of the metal from which it forms, tending to generate stresses within the oxide pockets, which promote development of a cracked, non-protective oxide. The cracked character of the oxide is evident from microscopy and metallography. The concentric crack structures suggest a series of uplifts as the oxide stresses apparently reached levels where shear could occur.

Stage c

As nodules begin to impinge on each other, they generate additional stresses and promote more cracking, further reducing the protective character of the oxide. However, progression to Stage c does not always occur at the same rates on a given material from one autoclave test to another, for reasons which are not clear.

Stage d

After complete nodule coalescence, a thick, relatively uniform oxide is generated. The oxide grows at rates which are much faster than the rates normally characteristic of Zircaloy oxidation at the test temperature (rates prior to nodule development). The most likely accelerating factor is stress. In a few cases, where uneven corrosion developed on two sides of a specimen at 500°C, substantial bending occurred, indicating that the oxide exerts major stresses. Some oxide spallation occurs in Stage d, though most of the oxide appears to remain on the specimen.

Stage e

Some specimens which develop nodular oxide survive for several autoclave cycles (many days) without complete oxidation. On other materials, almost complete oxidation to a pile of fine oxide particles can occur within 24 hours at 500°C. Stage e appears to be an outgrowth of Stage d. Again emphasizing an earlier observation, Stage e does not appear to have occurred in-reactor.

We have additional studies underway to develop a clearer understanding of the nodular phenomena which develop in the autoclave. Eventually we hope to relate that understanding to nodular phenomena which develop in-reactor.

Conclusions

1. Nodular corrosion phenomena which develop on Zircaloy components in BWR environments and to lesser extent on PWR components provide an incentive to understand the factors which promote them and development of methods to minimize them.

2. Nodular corrosion phenomena develop reproducibly on cold worked or extruded Zircaloy-2 and Zircaloy-4 specimens in Battelle Northwest autoclaves in high-pressure steam (1500-1700 psi) at 475°C and 500°C.

3. Alpha + beta and beta anneals followed by fast cooling were effective in suppressing the nodular attack on Zircaloy-2 and Zircaloy-4. Beta anneals followed by a slow cool induced a nodular attack. Alpha anneals were not reproducibly effective in suppressing nodules.

4. Preliminary evidence suggests that similarities exist in Zircaloy response to heat treatment and alloy factors in the autoclave and reactor environments. The autoclave test would become a useful screening tool if similar responses of materials to the two environments can be clearly demonstrated.

Acknowledgments

The authors are grateful to S.D. Deusser for operation of the autoclave equipment. The work was conducted under Energy Research and Development Administration (ERDA) Contract E(45-1)-1830. The temporary support of the ERDA-sponsored NORCUS[1] program for one of the co-authors (R.M. Horton) is gratefully acknowledged.

---

[1]Northwest College and University Association for Science

Figure List

Table List

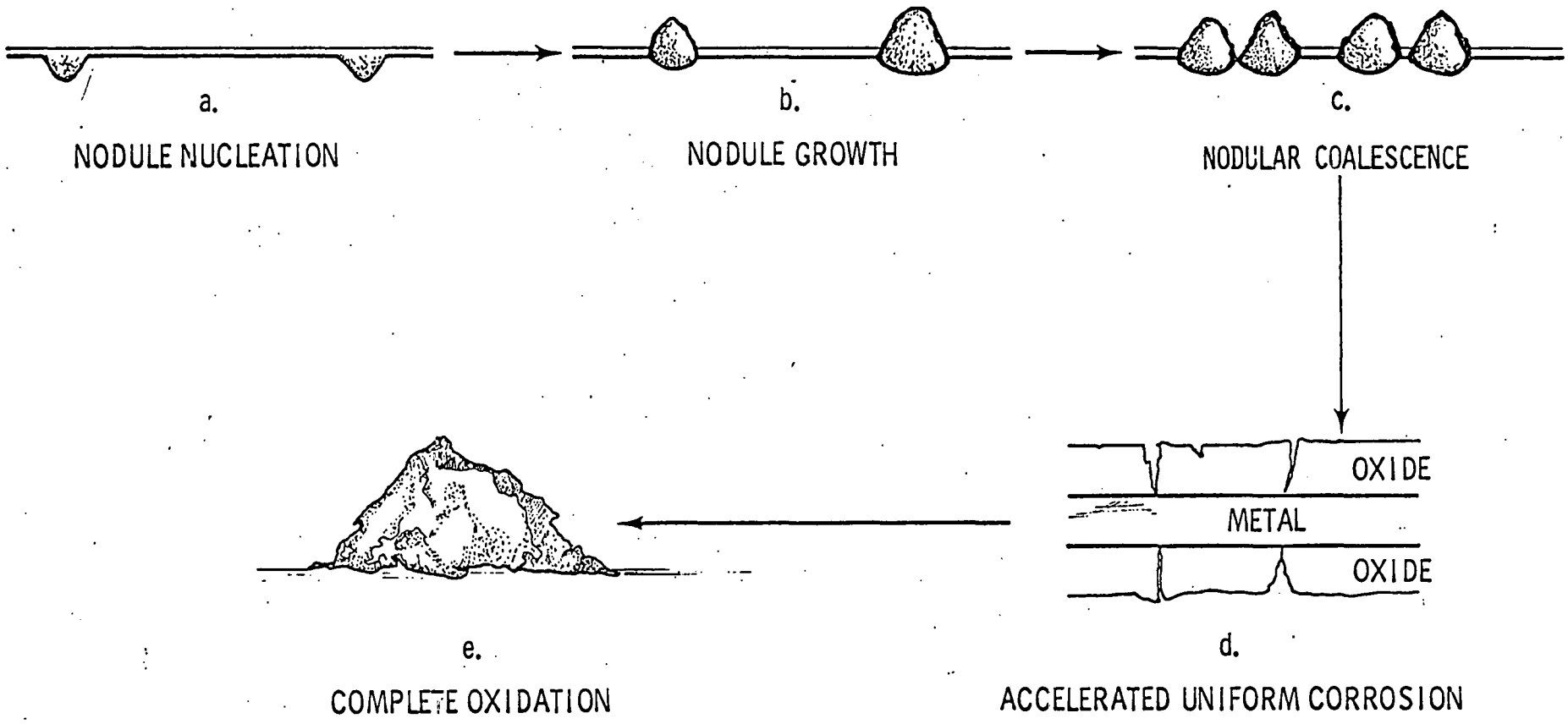

Figure 1 Stages of Nodular Corrosion

Metallurgical Conditions

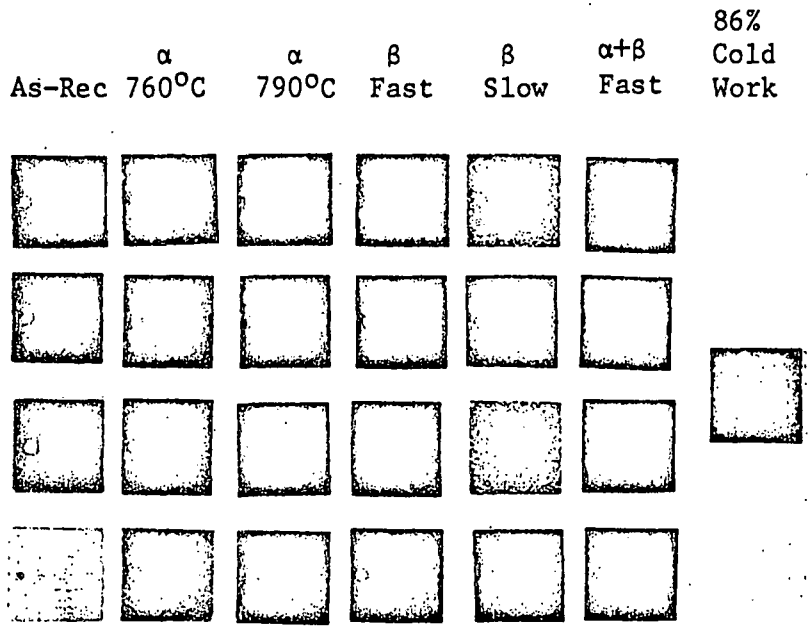

Figure 2 Zircaloy Coupons After 32 Hr. - 475°C, 1600 psig Steam

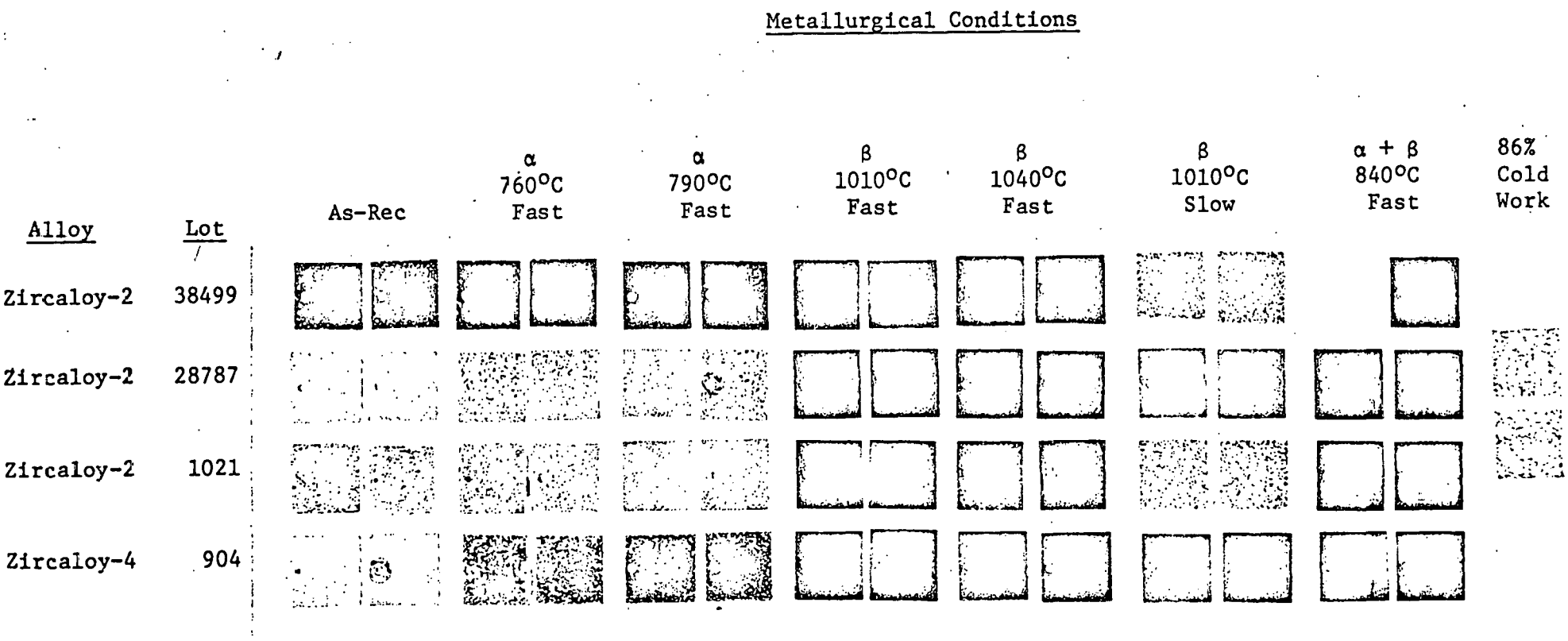

Figure 3 Zircaloy Coupons After 16 Hr. - 500°C, 1600 psig Steam

A

Neg. No. 4J 1002A 40X

Zircaloy-2 - As-Received - Lot 38449
Autoclaved - 500°C - 8 Hr.

B

Neg. No. 4J 1005A 40X

Zircaloy -4 - Alpha Ann - 790°C
Autoclaved - 500°C - 8 Hr.

C

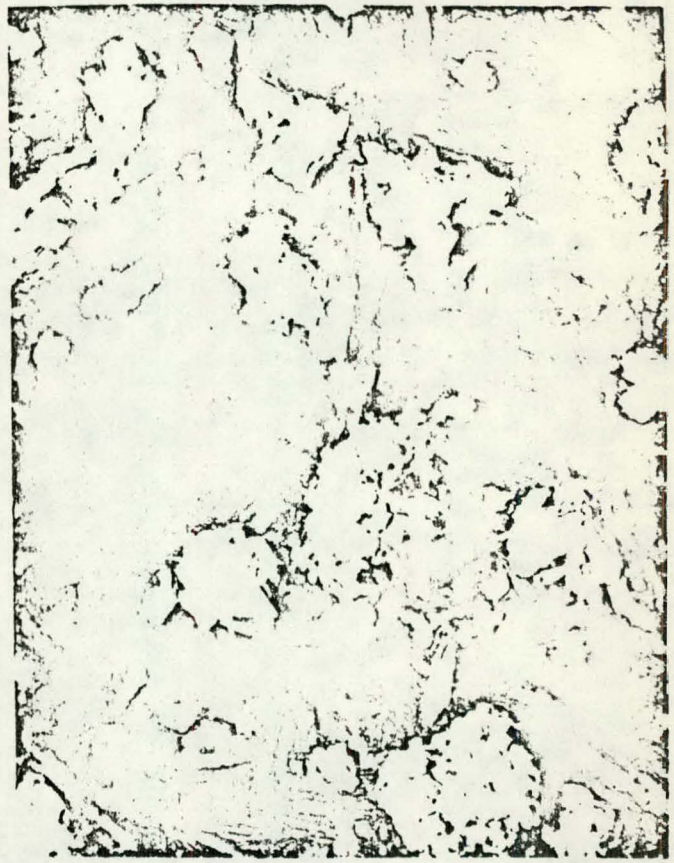

Neg. No. 4J 1008A 140X

Zircaloy-2 - βAnn - Slow Cool
Autoclaved - 500°C - 8 Hr.

Figure 4 Oxide Nodules - Top View

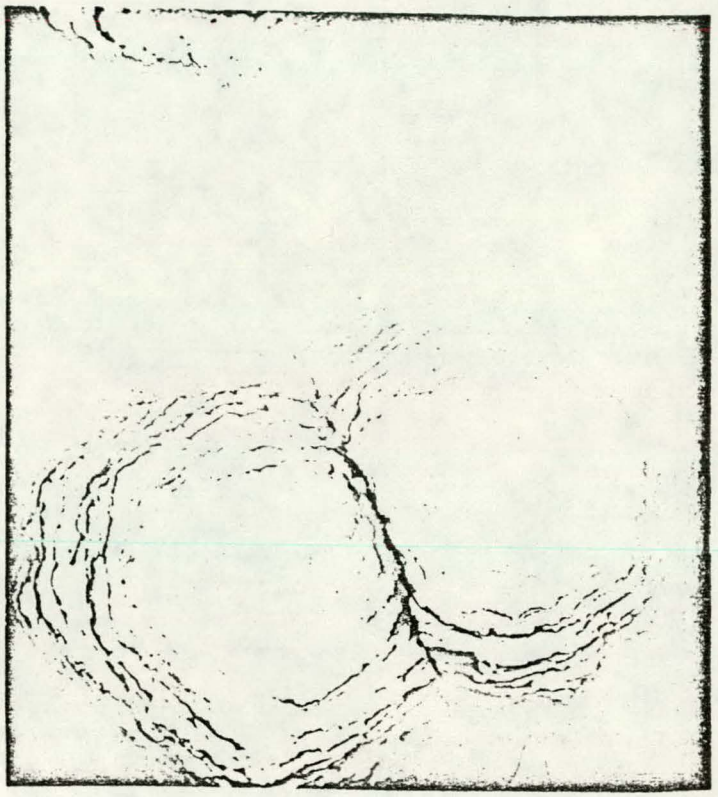

Neg. No. B1018 45X

Figure 5 Top View of Nodule Pair - SEM

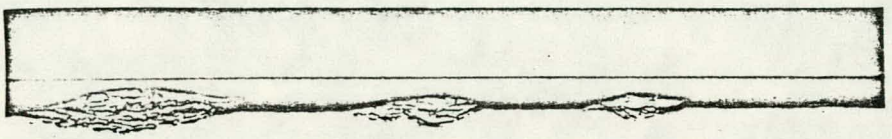

Neg. No. 4J 000 80X

Zircaloy-2	As-Rec	Lot 1021
Autoclave	500°C	8 Hr.

Figure 6. Cross Section of Oxide Nodules

Table 1 - Analysis of Alloys (Weight Percent)

	Zircaloy-2		Zircaloy-4
	Lot 38499 (a)	Lot 28787 (a)	Lot 1021 (a)	Lot 904 (b)
Sn	1.47	1.41	1.34	1.35
Fe	0.13	0.131	0.13	0.23
Cr	0.11	0.090	0.16	0.09
Ni	0.06	0.052	0.05	<0.0010
Al	0.0035	0.0035	0.0040	0.0025
C	0.0130	0.0170	0.0042	<0.0030
Cu	0.0014	<0.0020	0.0016	<0.0025
Hf	0.0062	0.0068	0.0090 (b)	<0.0077
H	0.0015	0.0020	0.0010 (b)	0.0017
N	0.0042	0.0040	0.0040	0.0034
O	0.108	0.118	--	--
Si	0.0052	0.0042	0.0030	0.0070
Ti	0.0034	0.0025	0.0010	<0.0020

(a) Analysis of sheet

(b) Highest analysis from top, middle and bottom of ingot

Table 2 - Heat Treatments Prior to Autoclaving

Description	Temp.(°C)	Time (hr)	Cooling Rate (b)
As Received (a)	-	-	-
Alpha	760	7	Fast
High Alpha	790	7	Fast
Beta I	1010	0.25	Fast
Beta II	1040	0.25	Fast
Beta I	1010	0.35	Slow
Alpha + Beta	840	0.7	Fast

(a) Zircaloy-2 Lot 38499 α vacuum annealed
Lot 28787 cold rolled
Lot 1021 cold rolled
Zircaloy-4 Lot 904 α vacuum annealed (1 hr. at 788°C)

(b) fast is approx. 10°C/sec. for T > 500°C; slow is 2.5°C/min.

Table 3 Weight Changes on Autoclaved Zircaloy - 475°C and 500°C

		Heat Treatment						
		As-Rec	Alpha		Alpha + Beta	Beta		
			760°C	790°C	840°C	1010°C (fast)	1040°C (fast)	1010°C (slow)
		mg/dm^2	mg/dm^2	mg/dm^2	mg/dm^2	mg/dm^2	mg/dm^2	mg/dm^2
Autoclaved 500°C, 16 Hr.:								
Zircaloy-2	Lot 38499	301	-	270	60	-	60	199
Zircaloy-2	Lot 28787	2735	-	1394	63	-	56	134
Zircaloy-2	Lot 1021	1912	-	2938	60	-	62	648
Zircaloy-4	Lot 904	2888	-	396	64	-	52	89
Autoclaved 475°C, 32 Hr.:								
Zircaloy-2	Lot 28499	50	50	53	41	44	32 (8 hr)	151
Zircaloy-2	Lot 28787	67	67	67	45	41	31 (8 hr)	103
Zircaloy-2	Lot 1021	64	44 (24 hr)	59	40	43	30 (8 hr)	161
Zircaloy-4	Lot 904	411	98	92	40	39	29 (8 hr)	71
Zircaloy-2	Lot HT 86% CW	99						

References

1. Megerth, F.H., Ruiz, C.P., and Wolff, U.E. Zircaloy-Clad UO_2 Fuel Rod Evaluation Program Final Report, November 1967-June 1971. USAEC Report GEAP 10371, General Electric Co., San Jose, Ca. June 1971.
2. Garzarolli, F., Diez, W., Franke, K.P., and Fricke, W. Proceedings, British Nuclear Energy Society Conference, London. July 1-2, 1971. P. 15.
3. Trowse, F.W. (cited in Ref. 4).
4. Lunde, Liv. Nuclear Engineering and Design, Vol. 33, 1975. pp. 178-195.
5. Dillon, R.L., and Johnson, A.B. Jr. "Corrosion Product Generation In Nuclear Reactors" Proceedings of the System Contamination Workshop, March 15-17, 1976, Atlanta, GA, pp. 67-80. Sponsored by Electric Power Research Institute, Palo Alto, CA.
6. Stehle, H., Kaden W., and Manzel, R. Nuclear Engineering and Design, Vol. 33, 1975, pp. 155-169.
7. Smalley, W.R., WCAP-3385, 1971.
8. Bain, A.S., and LeSurf, J.E. AECL-3065, 1969.
9. Dalgaard, S.B. "Long Term Corrosion and Hydriding of Zircaloy-4 Fuel Clad in Commercial Pressurized Water Reactors with Forced Convecture Heat Transfer," presented at the Electrochemical Society Meeting, May 2-7, 1976, Washington, D.C.
10. Johnson, A.B., Jr. ASTM STP 458, 1969, pp. 301-324.
11. Johnson, A.B., Jr., LeSurf, J.E., and Proebstle, ASTM STP 551, 1974, pp. 495-513.
12. Johnson, A.B., Jr. Reviews on Coatings and Corrosion Vol. 1 No. 4, 1975, pp. 299-365.
13. Johnson, A.B., Jr. Proceedings of the Fourth International Congress on Metallic Corrosion, 1969, Amsterdam, pp. 168-177.
14. Johnson, A.B., Jr. and Irwin, J.E., BNWL-463, 1967.
15. Van der Linde, A. Canadian Metallurgical Quarterly, Vol. 11, 1972, pp. 7-19.
16. Johnson, A.B., Jr. ASTM STP 458, 1969, pp. 271-285.
17. Cox, B. AECL-4448, 1973.
18. National Association of Corrosion Engineers Autoclaving Standard TM-01-71.